Laminated sediments from the central Peruvian continental slope: A 500 year record of upwelling system productivity, terrestrial runoff and redox conditions

Abdel Sifeddine, Dimitri Gutiérrez, Luc Ortlieb, Hugues Boucher, Federico Velazco, David Field, Gabriel Vargas, Mohammed Boussafir, Renato Salvatteci, Vicente Ferreira, et al.

Laminated sediments from the central Peruvian continental slope: A 500 year record of upwelling system productivity, terrestrial runoff and redox conditions

A. Sifeddine [a, i], D. Gutiérrez[b], L. Ortlieb[a], H. Boucher[a], F. Velazco[b], D. Field[c], G. Vargas[d], M. Boussafir[e], R. Salvatteci[b], V. Ferreira[f], M. García[a], J. Valdés[g], S. Caquineau[a], M. Mandeng Yogo[a], F. Cetin[a], J. Solis[b], P. Soler[h] and T. Baumgartner[f]

[a]IRD, Paleotropique (UR 055), 32 Avenue Henri Varagnat, 93143 Bondy Cedex, France

[b]IMARPE, Esquina Gamarra y General Valle s/n, Callao 22000, Peru

[c]Monterey Bay Aquarium Research Institute, 7700 Sandholdt Road, Moss Landing, CA 95039, USA

[d]Departamento de Geología, Facultad de Ciencias Físicas y Matemáticas, Universidad de Chile, Plaza Ercilla, Santiago, Chile

[e]Institut des Sciences de la Terre (ISTO), Université d'Orléans, 45067 Orléans, France

[f]CICESE, Km. 107 Carretera Tijuana – Ensenada 22860, Mexico

[g]Facultad de Recursos del Mar, Universidad de Antofagasta, Casilla 170, Antofagasta, Chile

[h]UMR LOCEAN, 5 Place Jussieu, 75005 Paris, France

[i]Departamento de Geoquimica, Universidade Federale Fluminense, RJ-Brasil

Abstract

Sedimentological studies including X-ray digital analyses, mineralogy, inorganic contents, and organic geochemistry on cores of laminated sediments accumulated in the oxygen minimum zone of the central Peruvian margin reveal variable oceanographic and climate conditions during the last 500 yr. Coherent upcore variations in sedimentological and geochemical markers in box cores taken off Pisco (B0405-6) and Callao (B0405-13) indicate that variability in the climate proxies examined has regional significance. Most noteworthy is a large shift in proxies at ~1820 AD, as determined by ^{210}Pb and ^{14}C radiometric dating. This shift is characterized by an increase in total organic carbon (TOC) in parallel with an abrupt increase in the enrichment factor for molybdenum Mo indicating a regional intensification of redox conditions, at least at the sediment water interface. In addition there was lower terrestrial input of quartz, feldspar and clays to the margin. Based on these results, we interpret that during several centuries prior to 1820, which corresponds to the little ice age (LIA), the northern Humboldt current region was less productive and experienced higher terrestrial input related to more humid conditions on the continent. These conditions were probably caused by a southward displacement of the inter-tropical convergence zone and the subtropical high pressure cell during the LIA. Since 1870, increases in TOC and terrigenous mineral fluxes suggest an increase of wind-driven upwelling and higher productivity. These

conditions continued to intensify during the late 20th century, as shown by instrumental records of wind forcing.

Keywords: Humboldt current system; Laminated sediments; Centennial variability; Recent Holocene; Paleoceanography

1. Introduction

The nearshore 200 km of Humboldt current system is strongly influenced by coastal upwelling and is one of the most productive marine ecosystems in the world (Pennington et al., 2006; Zuta and Guillén, 1970). Due to its large latitudinal extension, the upwelling varies in intensity and persistency during the year (Thomas et al., 1994). Off the Peruvian coast, near-continuous upwelling supports high rates of primary production and one of the world's largest fisheries. On the interannual time scale, oceanic circulation and upwelling is modulated by the El Niño-Southern Oscillation (ENSO) cycle, manifested as changes in near surface biological production (Arntz and Fahrbach, 1996) subsurface oxygenation, and terrestrial runoff to the nearshore ocean. Variability on decadal time-scales is observed in instrumental records (Chavez et al., 2003), but understanding the nature of longer-term change is hindered by the absence of long high-resolution records.

Paleoceanographic and paleoclimatic changes can be reconstructed from sedimentological variables, depending on preservation conditions during sedimentation and afterwards. Such variables are used as paleoenvironmental 'proxies', or indicators of past climate and ocean conditions. Preservation of paleoceanographic records is enhanced along portions of the Peruvian margin by occurrence of a strong subsurface oxygen minimum zone (OMZ; Helly and Levin, 2004) which inhibits biological 'reworking' of sediments. This OMZ extends from the southeast to the equatorial Pacific, and its formation and maintenance is supported by basin-scale circulation processes (Lukas, 1986) and high Humboldt current system (HCS) surface productivity and organic carbon fluxes from the surface into the OMZ, which amplify oxygen consumption in subsurface waters of the Peruvian coastal upwelling (PCU) system.

Paleoceanography of the continental shelves off South America has received little attention and climate over the last 1000 yr remains little studied (see [McCaffrey et al., 1990], [Rein et al., 2005] and [Gutiérrez et al., 2006]). Changes in temperature, salinity, and paleoproductivity have been examined however at glacial and interglacial time-scales ([Suess et al., 1990], [Fink et al., 2006] and [Rein, 2007]). Several sedimentary accumulation zones along the central Peruvian continental margin have favorable conditions to preserve past environmental events with high temporal resolution: bottom-water dysoxia, high sedimentation rates, and stable topographical settings ([Suess et al., 1990], [Reinhardt et al., 2002] and [Gutiérrez et al., 2006]). Gutiérrez et al. (2006) constructed detailed paleoceanographic records of the past several centuries from laminated sediments from the central Peruvian margin. The combination of high productivity and near-anoxic conditions over the Peruvian margin results in the preservation of annual to decade-scale variations in climate and upwelling in organic and inorganic geochemical proxies ([Krissek and Scheidegger, 1983], [Suess et al., 1990], [Böning et al., 2004] and [McManus et al., 2006]).

Here we use mineral content and organic and inorganic markers in sediment cores to examine, at different time-scales, past changes in productivity, sediment redox conditions and terrigenous input (Table 1). We use total organic carbon (TOC) to infer productivity, and an oxygen index (OI) to infer degree of aerobic oxidation of TOC. Redox-sensitive metals (e.g.

molybdenum) can be used to indicate redox conditions in the sedimentary environment at the time of deposition. This particular behavior has permitted reconstruction of past bottom-water oxygenation based on molybdenum (Mo) concentration profiles in sediment cores ([McManus et al., 2006], [Tribovillard et al., 2006] and [Tribovillard et al., 2008]). Finally, the mineralogical composition of sediment cores can provide information on past conditions by recording terrigenous input as related to erosion, aeolian transport, runoff, and deposition onto continental shelf ([Vargas et al., 2004] and [Rein, 2007]).

2. Oceanographic setting

Coastal upwelling occurs along the eastern margins of major oceanic basins when predominantly along-shore winds and Coriolis force drive surface waters offshore and these are replaced by deeper, cooler and nutrient-rich waters. The enhanced biological productivity supported by upwelling increases the flux of organic material to the coastal ocean floor. This flux intensifies the OMZ and results a high rate of TOC deposition on the continental shelves, both of which limit organic matter degradation and favor preservation. As a consequence the organic carbon content of sediments beneath upwelling systems may reach 10% ([Libes, 1992] and [Hedges and Keil, 1995]), whereas organic carbon in sediments beneath oligotrophic oceans typically varies from 0.2% to 0.4% ([Muller and Suess, 1979] and [Duan, 2000]).

Upwelling-favorable along-shore winds are present along the Peruvian coast all year long and maximal between 14°S and 16°S, weakening in the north, near Punta Falsa (6°S; Echevin et al., 2004). Wind strength however varies and ‘upwelling events’ last from a few days to a week and are stronger and more frequent in winter due to offshore winds associated with a strengthened subtropical high pressure cell. The wind-driven surface circulation consists in a shallow, equatorward, coastal jet (Strub et al., 1998), with maximum intensity in winter, known as the Peruvian coastal current. This current can be identified by the shoaling of isopycnals in the nearshore surface layers. Offshore, the circulation is dominated by poleward flows, identified as the Peru–Chile counter current which advects warm and saline waters from tropical origin (Lukas, 1986). Below the surface coastal current, the subsurface, coastally trapped, Peru–Chile undercurrent advects saline (35.0–35.1 PSU) tropical waters poleward. Its signature is characterized by the deepening of isopycnals towards the coast at 50–200 m depth (Echevin et al., 2004).

Off the central Peruvian coast (9–15°S), the upper margin sediments are organic-rich. Excess ^{210}Pb-derived sedimentation rates vary from 0.04 to 0.15 cm yr^{-1} ([Reimers and Suess, 1983] and [Levin et al., 2003]). Based on exploratory surveys and literature, the Callao (~12°S) and Pisco (~14°S) areas were selected as sample sites. Two Soutar-box cores were collected in May 2004 by the R/V Olaya (Instituto del Mar del Peru, IMARPE): The first one from the continental shelf off Callao (B0405-13, 12°00′S, 72°42′S, 184 m water-depth); and the second one from the upper continental slope off Pisco (B0405-06, 14°07′S, 76°30′S, 299 m water-depth; Gutiérrez et al., 2006; Fig. 1).

3. Analytical procedures

Sedimentary structures were documented by X-radiography (SCOPIX, Migeon et al., 1999). Chronological models for the last 130 yr were developed by using the downcore distributions of natural excess ^{210}Pb and ^{230}Th and of the bomb-derived ^{241}Am. The chronology beyond the

last 130 yr was inferred from radiocarbon ages, calibrated with local reservoir effects by Gutiérrez et al. (2008).

Mineralogical composition was obtained by X-ray diffraction (XRD) and by Fourier transformed infrared spectrometry (FTIR) respectively. For FTIR analyses, samples were placed in a KBr disc, which ensures that Lambert–Beer's law is valid. A quantitative determination of the mineral content from various blends was performed by making a multi-component analysis of the experimental spectrum using the spectra of each component in the mixture (Bertaux et al., 1998). Mean relative standard deviation was 0.8% for the mineral quantification.

Organic matter characterization and quantification were done using Rock-Eval 6 programmed pyrolysis (Lafargue et al., 1998). Total organic carbon (TOC %) reflects the quantity of organic matter (OM) present in the sediment. Normalized to TOC the hydrogen index is the amount of hydrocarbon (HC) released during pyrolysis (HI, mg HC/g TOC), and the oxygen index similarly gives the oxygen content calculated from the amounts of CO and CO_2 released during pyrolysis (OI, OIRe6, mg O_2/g TOC).

Molybdenum (Mo) and Aluminium (Al) concentrations were analysed by ICP-MS (Ultramass Varian) and ICP-AES, respectively, after hot-plate acid digestion (combination of acids: HF, $HN0_3$, $HClO_4$) which eliminated organic matter and removed silicates ([Zwolsman and Van Eck, 1999] and [Cho et al., 1999]). Measurement precision for Al and Mo was determined by comparing duplicate analyses (usually ±0.04% and ±0.03% respectively).

Mo is a trace metal used to asses past redox conditions ([Tribovillard et al., 2006], [Tribovillard et al., 2008] and [McManus et al., 2006]). As a redox-sensitive metal, Mo is commonly removed from the ocean and transferred to the sediments via different pathways ([McManus et al., 2006], [Poulson et al., 2006], [Tribovillard et al., 2006] and [Tribovillard et al., 2008]). In oxic sediments, where aerobic respiration decomposes organics, Mo is scavenged from the water column with an association of metal oxides. Under reducing conditions however, where anaerobic processes dominate, Mo is removed from the water column with sulfidized organic material or via sequestration by Fe–S phases. Sediments contain variable amounts of biogenic materials that dilute the trace-elements, most commonly calcium carbonate and opal. Thus, to compare trace-element proportions in samples that contain varying carbonate and opal contents, it is customary to normalize trace-element (here Mo) concentrations to Al content (Tribovillard et al., 2006). Al is a constituent of the aluminosilicate fraction of the sediments and is essentially inert during diagenesis. Moreover, according to Valdés et al. (2005), Al normalization enables regional comparison and the evaluation of terrestrial input of trace metals. The method is also applied to determine Enrichment Factors (EFs) according the equation described by Tribovillard et al. (2006): $EF = (Mo/Al)_{sample}/(Mo/Al)_{average\ shale}$). We used values for average shales from different sources ([Turekian and Wedepohl, 1961] and [McManus et al., 2006]). If Mo EF is greater than 1, then Mo is enriched relative to average shales and, if Mo EF is less than 1, it is depleted.

The particulate fluxes for each sediment constituent (TOC, quartz, feldspar and clays) are calculated by multiplying the concentration of each constituent by the overall sediment accumulation rate. In general terms, this relation can be expressed as: sediment flux (mg cm^{-2} yr^{-1}) = element concentration (mg g^{-1}) × sediment accumulation rate (g cm^{-2} yr^{-1}).

The flux estimation for each element has the advantage of providing information on the inputs of the different constituents independently of their relative dilution in the matrix.

Thin sections were constructed from resin-impregnated 10 cm longitudinal segments of the Callao core (B0405-13). Water was replaced by acetone prior to impregnation with resin following Bénard (1996) and Zaragosi et al. (2006). After impregnation with resin, the bonded blocks were cut to approximately 100 μm using a precision saw (ESCIL LT-260) and thereafter hand polished to a thickness of 30 μm using the rotating lapidary unit. Finally, cover slips were fixed on the thin sections using the collage resin mixture. The structure of the laminations was analysed using a polarised light microscope, with a magnification of 20.

In order to estimate the shared variability of the environmental proxies and their relationships with one another, we applied a principal component analysis (PCA).

4. Results

4.1. Lithology and chronology

The observation of the core X-ray images reveals the existence of bands and laminations (<5 mm thickness), formed by the succession of light (dense) and dark (less dense) layers, which appear to have been deposited with negligible bioturbation under nearly anoxic conditions (Fig. 1). Three stratigraphic units are observed in the Pisco Core. The basal unit (unit I) (74–62 cm) is formed by the succession of several primarily banded sediments. The unit II, which starts at 62 cm and extends to 34 cm, presents a slump at the base (55–52 cm). This unit, which is characterized by an overall greater density (lightly colored in the X-radiograph; Fig. 1), contains pairs or 'couplets' of dark and light laminae that range from 2 to 5 mm in thickness. The upper unit (unit III) (34–0 cm), with average lower density (darker in Fig. 1), is marked by a series of thick light and dark band (ca. 1 cm). In the Callao core, the X-ray image also reveals three units that are similar to those of the Pisco core in density and depth. Unit I (84–66 cm) also contains band structures. Unit II (66–34 cm) is denser (lighter color), as in the Pisco core, but is formed by thick bands (~1 cm) rather than fine laminations as observed in the Pisco core and is interrupted by several slumps in the middle part of the unit. Unit III (34–0 cm) is marked by a low density and is formed by the succession of both millimeter-thick laminae and broader bands.

Average sedimentation rates are ~2.2 mm yr^{-1} for the Pisco core and ~2.1 mm yr^{-1} for the Callao core for the lapse 1870 AD to present. The centuries prior to the late 19th century have average sedimentation rates of 1 and 0.6 mm yr^{-1}, respectively (Gutiérrez et al., 2008). At these rates the banding patterns in Fig. 1 do not resolve interannual or even decadal-scale variability (and can be affected by water content and compaction from burial; Gutiérrez et al., 2008). The results are presented as concentrations (%) and fluxes of sediment constituents.

4.2. Mineral fraction

X-ray diffraction (XRD) shows that the terrigenous mineral fraction of both cores is quartz, feldspar, kaolinite, illite and vermiculite. The upcore variations in these fractions are similar in both cores (Fig. 2) and identify three sections which correspond to the units identified through the XRD lithological description of Fig. 1.

Unit I (prior to 1400 AD) is characterized by low quartz, feldspar and clays content (respective mean abundances of 6%, 10% and 10%). Unit II (~1400–1820 AD) begins with an increase of quartz (5–15%), feldspar (10–20%) and clays (10–28%). Concentrations remain relatively stable until the top of the unit. Unit III (1820–2004 AD) starts with a decrease in concentrations of quartz, feldspar and clays that reach minimum values and then increase to the top of this unit reaching values around 10%, 15% and 20%, respectively.

In both cores the variations in upcore fluxes (Fig. 3) are similar to the variations in percent composition (Fig. 2), and again correspond to the three different stratigraphic units. Before 1400 AD fluxes of quartz, feldspar and clays were low around 2, 2 and 4 mg cm^{-2} yr^{-1}, respectively. Between 1400 and 1820 AD fluxes of quartz, feldspar and clays were high around 4, 3 and 6 mg cm^{-2} yr^{-1}, respectively. Over 1820–1870, fluxes of quartz (4–0.5 mg cm^{-2} yr^{-1}), feldspar (3–1 mg cm^{-2} yr^{-1}) and clays (6–1 mg cm^{-2} yr^{-1}) decreased abruptly. Finally over 1870–2004 AD, fluxes of quartz, feldspar and clays steadily increased, beginning around 1870 AD and intensifying around 1950 AD with values around 6, 7 and 8 mg cm^{-2} yr^{-1}, respectively, in the superficial sediments.

4.3. Inorganic fraction

Upcore variations in Al are similar to the variability in clays described above (Fig. 2). Al values are somewhat low (3%) during the first unit and then increase, reaching 5% in unit II. In unit III, Al initially decreases to ~ 1% around 1870 (1%), and then steadily increases to 6% towards the top of unit III.

Variations in Mo (mg kg^{-1}) are similar to the minerals above only into unit III (Fig. 2). Mo fluctuates around 75 (mg kg^{-1}) before 1400 AD (Unit I) and later decreases and stabilizes around 25 mg kg^{-1} through unit II. In the unit III (1820–2004 AD), Mo increases steadily to 75 mg kg^{-1}.

The Mo enrichment factor in both cores is >1 suggesting a non-terrigenous origin for this metal. The upcore variation in EF for Mo is similar to the variability in mineral fractions only for unit III (Fig. 3). In unit I Mo EF is around 120; and in unit II, it decreases to ~ 50. Mo EF increases in both cores in unit III, although Callao has a much higher maximum EF than the Pisco core (500 vs. 300). In general, Mo EF values are moderate in the Callao core from 1870 to 2004 AD and in the Pisco core from 1820 to 2004 AD.

4.4. Organic fraction

Upcore variations in TOC correspond to the sedimentological and mineralogical records into Unit III of both cores (Fig. 2). TOCs are near 5% in units I and II of both cores and the OI varies between 120 and 80 for the Pisco and Callao cores, respectively. There is a large increase in TOC within unit III, with higher values in the Callao core (16%) than in the Pisco core (12%). This trend in TOC is accompanied by a progressive decrease in OI towards the core tops, reaching values around 80 in the Pisco core and 70 in the Callao core. TOC fluxes exhibit low values in unit I in both cores (~ 1.2 mg cm^{-2} yr^{-1}). A transient increase in TOC flux occurs around 1820 AD, associated with decreases in quartz and other minerals fluxes. A positive trend in TOC flux starts at ~1870 AD, reaching ~ 4 and ~ 6 mg cm^{-2} yr^{-1}, at Pisco and Callao, respectively, in the 2000s.

4.5. Principal component analysis

A principal component analysis was run on the upcore constituents from each core. Concentrations were used rather than fluxes since uncertainties in chronology can affect estimated flux rates. In particular, if the change in sedimentation rates reported at 1870 is associated with changes in TOC, then the period 1820–1850 AD may have much higher sedimentation rates and consequently, higher fluxes of TOC and other constituents than calculated. At each site, more that 85% of variance is explained by two principal components (Fig. 4). Here, we present only the first component (PC1), which is a negative correlation between the terrigenous fraction (quartz, feldspar, clays and aluminum) and TOC and Molybdenum (Fig. 4).

5. Discussion

The parallel upcore variations of PC1 (Fig. 5) in the Pisco and Callao sites indicate that the environmental proxies exhibit the same pattern in both cores and thus have at least regional significance. The shift at ~ 1820 AD in both the stratigraphic observations and sedimentological constituents is much stronger than the change at the base of the cores (division between units I and II), which is not apparent in all proxies. A large climatic change apparently occurred at ~1820 AD, which was of greater magnitude than other climate fluctuations throughout the last several centuries. Nevertheless, noteworthy sedimentological fluctuations occur within unit III.

5.1. Little ice age period

High mineral fluxes characterize the 1400–1820 AD period which corresponds to the little ice age (LIA), or rather its South-American counterpart. Examination of thin sections from the Callao core prior to 1820 AD shows that most terrigenous particles (quartz and feldspar; 50–80 μm) present angular to sub-angular aspects, suggesting a fluvial source (Fig. 1) rather than aeolian transport. Similarly, Pisco core particle morphology prior to 1820 suggests river discharge. The similar patterns of flux at both sites are interpreted as resulting from substantial terrestrial input followed by dispersion and transport by the coastal circulation in unit II.

The negative values of PC1 (Fig. 5) during the little ice age (Unit II) reflect both the high mineral content and low Mo content (Fig. 3). Sediments rich in Mo characterize the upper Peruvian margin (<300 m) with high sulphate reduction rates (Böning et al., 2004) under anoxic conditions (see [Valdés et al., 2005], [McManus et al., 2006], [Tribovillard et al., 2006] and [Tribovillard et al., 2008]). Low Mo content during the LIA is probably due to reduced organic loading and suboxic conditions in the surficial sediments.

The LIA period thus appears marked by a low productivity, suboxic sediments and higher terrestrial input of minerals related to rainfall and runoff from the continent. In the Cariaco basin (Venezuela) ([Haug et al., 2001] and [Peterson and Haug, 2006]), drier conditions are suggested for the LIA by decreased Ti content in cores linked to decreased detritus from local rivers. Hence, our results are consistent with a global southward migration of the inter-tropical convergence zone (ITCZ), as postulated also by Graham et al. (2007) and Newton et al. (2006).

At seasonal and interannual time-scales, an ITCZ southward shift is associated with the southward projection of surface nutrient poor Equatorial and Tropical water masses. An additional consequence of a southward shift in the ITCZ would be a reduced strength of the subtropical high pressure system that produces upwelling favorable winds. In turn these modifications may cause reductions in coastal upwelling, primary production, and flux of organic material to the continental slope, as observed in the Callao and Pisco cores (Gutiérrez et al., 2008). Note that the variability of efficiency factor (EF) for Mo is inversely related with terrestrial fluxes, suggesting sediment redox conditions changes, which are associated to the organic matter flux changes. This regional response is likely a result of the establishment of new ocean–atmosphere connections that control the position of the ITCZ.

5.2. The modern period

The simultaneous decrease of terrigenous fluxes after 1820 in both cores probably marks a change from rainy to drier conditions. The increase of Mo enrichment factor, in the same period, suggests an enhancement of sediment redox conditions linked to the establishment of a new ocean–atmosphere connection pattern. A transient decrease of TOC flux and an increase of OI are recorded during the lapse 1845–1865 AD. After these two decades, carbon flux exhibits a positive trend while OI decreases, thus suggesting less oxidation of the settling organic matter. This trend coincides with an increase of the dominance of anoxia-tolerant taxa in the benthic foraminiferal assemblage at Pisco, as reported by Morales et al. (2006). Increases in TOC flux are also recorded during the same period in sediments from the continental slope 15°S (McCaffrey et al., 1990) and from Mejillones Bay at 23°S ([Valdés et al., 2004], [Vargas et al., 2004] and [Vargas et al., 2007]). These results indicate a regional centennial enhancement of productivity and organic particles export to the sediment. An intensification of this trend is observed since mid-twentieth century, which is likely caused by enhanced upwelling, as recorded instrumentally during the same period (Jahncke et al., 2004; Fig. 6).

6. Conclusion

Laminated sediments from the central Peru continental slope, accumulated under intense upwelling, dysoxia and high sedimentation rates, preserve and record different oceanographic and climatic changes during the last 500 yr. The measurement of different organic, mineral and inorganic variables in cores provides environmental proxies linked to (1) upwelling and productivity, (2) strength of the sediment redox conditions, and (3) terrigenous input to sediments. Changes in the terrigenous input likely correspond to changes in continental rainfall, which affects mineral-laden runoff that is subsequently deposited offshore. A comparison with Cariaco Basin core records of regional precipitation and runoff supports our interpretation that during the little ice age before 1820, the inter-tropical convergence zone (ITCZ) likely occupied a more southerly position and that more humid conditions prevailed in Peru. A more southerly ITCZ would also correspond to a reduced subtropical high pressure system with weaker along-shore winds, and lower primary productivity. Conversely, since the late nineteenth century, increasing TOC fluxes and sediment anoxia are interpreted as caused by the intensification of coastal upwelling, productivity and organic particles delivery to the bottom.

Acknowledgements

This study was supported by the IRD PALEOTROPIQUE research unit (UR 055) and the IMARPE PALEOMAP research program, as well as by the PALEOPECES project (IMARPE-IRD), the IAI small grant project SGP 211-222 (PI: D. Gutiérrez), the Humboldt current system program (ATI-IRD) and finally the PCCC project (French national research agency ANR, P.I. B. Dewitte). We thank the Instituto del Mar del Peru (IMARPE) for full support of this research and acknowledge the crew of the RV José Olaya Balandra and other scientific participants in the box-coring survey.

The authors thank anonymous reviewers and the editors of the special issue for their help in the improvement of the manuscript.

References

Arntz and Fahrbach, 1996 W. Arntz and E. Fahrbach, *El Niño: experimento climático de la naturaleza*, *Causas físicas y efectos biológicos*, Fondo de Cultura Económica, México, D.F (1996) 309 p.

Bénard, 1996 Y. Bénard, Les techniques de fabrication des lames minces de sol, *Cahiers Techniques Institut Nationale de Recherche Agronomique* **37** (1996), pp. 29–42.

Bertaux et al., 1998 J. Bertaux, F. Frohlich and Ph. Ildefonse, Multicomponent analysis of FTIR spectra: quantification of amorphous silica and crystallized mineral phases in synthetic and natural sediments, *Journal of Sedimentary Research* **68** (3) (1998), pp. 440–447.

Böning et al., 2004 Ph. Böning, H.J. Brumsack, M.E. Böttcher, B. Schnetger, C. Kriete, J. Kallmeyer and S.L. Borcher, Geochemistry of Peruvian near-surface sediments, *Geochimica et Cosmochimica Acta* **68** (2004), pp. 4429–4451

Chavez et al., 2003 F.P. Chavez, J. Ryan, S.E. Lluch-Cota and M.C. Ñiquen, From anchovies to sardines and back-multidecadal change in the Pacific Ocean, *Science* **299** (2003), pp. 217–221.

Cho et al., 1999 Y. Cho, C. Lee and M. Choi, Geochemistry of surface sediments off the southern and western coast of Korea, *Marine Geology* **159** (1999), pp. 111–129.

Duan, 2000 Y. Duan, Organic geochemistry of recent marine sediments from the Nansha Sea China, *Organic Geochemistry* **31** (2000), pp. 159–167.

Echevin et al., 2004 V. Echevin, I. Puillat, C. Grados and B. Dewitte, Seasonal and mesoscale variability in the Peru upwelling system from in situ data during the years 2000 to 2004, *Gayana Concepcion* **68** (2004), pp. 167–173 ISSN 0717-6538.

Fink et al., 2006 Fink, D., Skilbeck, G., Gagan, M., 2006. A 25,000 year inter-annual record of the Peru–Chile current and implications for ENSO variation during deglaciation. In: Nineteenth International Radiocarbon Conference, Oxford April 3–7, 2006, p.174.

Graham et al., 2007 Graham, N.E., Hugues, M.K., Ammann, C.M., Cobb, K.M., Hoerling, M.P., Kennett, D.J., Kennett, J.P., Rein, B., Stott, L., Wigand, P.E., Xu, T., 2007. Tropical

Pacific – mid-latitude teleconnections in the medieval times. Climatic Change 83, 241–285. doi 10.1007/s10584-007-9239-2.

Gutiérrez et al., 2006 D. Gutiérrez, A. Sifeddine, J.L. Reyss, G. Vargas, R. Salvatteci, V. Ferreira, L. Ortlieb, D. Field, T. Baumgartner, M. Boussafir, H. Boucher, J. Valdes, L. Marinovic, P. Soler and P. Tapia, Anoxic sediments off central Peru record interannual to multidecadal changes of climate and upwelling ecosystem during the last two centuries, *Advances in Geosciences* **6** (2006), pp. 119–125.

Gutiérrez et al., 2008 D. Gutiérrez, A. Sifeddine, D.B. Field, L. Ortlieb, G. Vargas, F. Chávez, F. Velazco, V. Ferreira, P. Tapia, R. Salvatteci, H. Boucher, M.C. Morales, J. Valdés, J.L. Reyss, A. Campusano, M. Boussafir, M. Mandeng-Yogo, M. García and T. Baumgartner, Rapid reorganization in ocean biogeochemistry off Peru towards the end of the little ice age, *Biogeosciences Discuss* **5** (2008), pp. 3919–3943.

Haug et al., 2001 G.H. Haug, K.A. Hughen, D.M. Sigman, L.C. Peterson and U. Röhl, Southward migration of the intertropical convergence zone through the Holocene, *Science* **293** (2001), pp. 1304–1308.

Hedges and Keil, 1995 J. Hedges and R. Keil, Sedimentary organic matter preservation, an assessment and speculative synthesis, *Marine Chemistry* **49** (1995), pp. 81–115.

Helly and Levin, 2004 J. Helly and L. Levin, Global distribution of naturally occurring marine hypoxia on continental margins, *Deep-Sea Research I* **51** (2004), pp. 1159–1168.

Jahncke et al., 2004 J. Jahncke, D. Checkley and G.L. Hunt, Trends in carbon flux to seabirds in the Peruvian upwelling system: effects of wind and fisheries on population regulation, *Fisheries Oceanography* **13** (2004), pp. 208–223.

Krissek and Scheidegger, 1983 L.A. Krissek and K.F. Scheidegger, Environmental controls on sediment texture and composition in low oxygen zones off Peru and Oregon. In: E. Suess and J. Thiede, Editors, *Coastal Upwelling; Its Sediment Record. Part B: Sedimentary Records of Ancient Coastal Upwelling*, Plenum Press, New York (1983), pp. 63–180.

Lafargue et al., 1998 E. Lafargue, F. Marquis and D. Pillot, Rock-Eval 6 applications in hydrocarbon exploration, production, and soil contamination studies, *Revue de l'Institut Français du Pétrole* **53** (4) (1998), pp. 421–437

Levin et al., 2003 L.A. Levin, A.E.R. Rathburn, D. Gutiérrez, P. Muñoz and A. Shankle, Bioturbation by symbiont-bearing annelids in near-anoxic sediments: implications for biofacies models and paleo-oxygen assessments, *Palaeogeography, Palaeoclimatology, Palaeoecology* **199** (2003), pp. 120–140.

Libes, 1992 S. Libes, An Introduction to Marine Biogeochemistry, John Wiley & Sons, Inc., New York (1992) 289 p.

Lukas, 1986 R. Lukas, The termination of the equatorial undercurrent in the eastern Pacific, *Progress in Oceanography* **16** (1986), pp. 63–90.

McCaffrey et al., 1990 M.A. McCaffrey, J.W. Farrington and D.J. Repeta, The organic geochemistry of Peru margin surface sediments: I. A comparison of the C3, alkenone and historical El Niño records, *Geochimica et Cosmochimica Acta* **54** (1990), pp. 1671–1682.

McManus et al., 2006 J. McManus, W.M. Berelson, S. Severmann, R.L. Poulson, D.E. Hammond, G.P. Klinkhammer and Ch. Holm, Molybdenum and uranium geochemistry in continental margin sediments: paleoproxy potential, *Geochimica et Cosmochimica Acta* **70** (2006), pp. 4643–4662

Migeon et al., 1999 S. Migeon, O. Weber, J.-C. Faugères and J. Saint-Paul, SCOPIX: a new X-ray imaging system for core analysis, *Geo-Marine Letters* **18** (1999), pp. 225–251.

Morales et al., 2006 M.C. Morales, D. Field, S.M. Pastor, D. Gutiérrez, A. Sifeddine, L. Ortlieb, V. Ferreira, R. Salvatteci and F. Velazco, Variations in foraminifera over the last 460 years from laminated sediments off the coast of Peru, *Boletin de la Sociedad Geológica del Perú* **101** (2006), pp. 5–18.

Muller and Suess, 1979 P. Muller and E. Suess, Productivity, sedimentation rate, and sedimentary organic matter in the ocean – I. Organic carbon preservation, *Deep-Sea Research* **26A** (1979), pp. 1347–1362.

Newton et al., 2006 A. Newton, R. Thunell and L. Stott, Climate and hydrographic variability in the Indo-Pacific Warm Pool during the last millennium, *Geophysical Research Letters* **33** (2006), p. L19710

Pennington et al., 2006 J.T. Pennington, K.L. Mahoney, V.S. Kuwahara, D.D. Kolber, R. Calienes and F.P. Chavez, Primary production in the eastern tropical Pacific: a review, *Progress in Oceanography* **69** (2006), pp. 285–317.

Peterson and Haug, 2006 L.C. Peterson and G.H. Haug, Variability in the mean latitude of the Atlantic intertropical convergence zone as recorded by riverine input of sediments to the Cariaco Basin (Venezuela), *Palaeogeography, Paeoclimatology, Palaeocology* **243** (2006), pp. 97–113.

Poulson et al., 2006 R.L. Poulson, Ch. Siebert, J. McManus, M. William and W.M. Berelson, Authigenic molybdenum isotope signatures in marine sediments, *Geology* **34** (2006), pp. 617–620.

Reimers and Suess, 1983 C.E. Reimers and E. Suess, Spatial and temporal patterns of organic matter accumulation on the Peru continental margin. In: J. Thiede and E. Suess, Editors, *Coastal Upwelling: Its Sediment Record. Part B: Sedimentary Records of Ancient Coastal Upwelling*, Plenum, New York (1983), pp. 311–346.

Rein, 2007 B. Rein, How do the 1982/83 and 1997/98 El Niños rank in a geological record from Peru, *Quaternary International* **161** (2007), pp. 56–66.

Rein et al., 2005 B. Rein, A. Lückge, L. Reinhardt, F. Sirocko, A. Wolf and W.C. Dullo, El Niño variability off Peru during the last 20,000 years, *Paleoceanography* **20** (2005)
.

Reinhardt et al., 2002 L. Reinhardt, H.-R. Kudrass, A. Lückge, M. Wiedicke, J. Wunderlich and G. Wendt, High-resolution sediment echo-sounding off Peru: Late Quaternary depositional sequences and sedimentary structures of a current-dominated shelf, *Marine Geophysical Research* **23** (2002), pp. 335–351.

Strub et al., 1998 P.T. Strub, J.M. Mesías, V. Montecino and J. Rutllant, Coastal ocean circulation off western South America. In: A.R. Robinson and K.H. Brink, Editors, *The Sea 11, The Global Coastal Ocean*, Interscience, New York (1998), pp. 273–313.

Suess et al., 1990 E. Suess and R. Von Huene *et al.*, Proceedings of the ocean drilling program, *Scientific Results* **112** (1990), p. 738.

Thomas et al., 1994 A.C. Thomas, F. Huang, P.T. Strub and C. James, Comparison of the seasonal and interannual variability of phytoplankton pigment concentrations in the Peru and California Current systems, *Journal of Geophysical Research* **99** (1994), pp. 7355–7370.

Tribovillard et al., 2006 N. Tribovillard, Th. Algeo, T. Lyons and A. Riboulleau, Trace metals as paleoredox and paleoproductivity proxies: an update, *Chemical Geology* **232** (2006), pp. 12–32

Tribovillard et al., 2008 N. Tribovillard, T.W. Lyons, A. Riboulleau and V. Bout-Roumazeilles, A possible capture of molybdenum during early diagenesis of dysoxic sediments, *Bulletin de la Societé Géologique de France* **179** (2008), pp. 3–12.

Turekian and Wedepohl, 1961 K. Turekian and K. Wedepohl, Distribution of the elements in some major units of the earth's crust, *Geological Society of America Bulletin* **72** (1961), pp. 175–192.

Valdés et al., 2004 J. Valdés, A. Sifeddine, E. Lallier-Verges and L. Ortlieb, Petrographic and geochemical study of organic matter in surficial laminated sediments from an upwelling system (Mejillones del Sur Bay, northern Chile), *Organic Geochemistry* **35** (2004), pp. 881–894.

Valdés et al., 2005 J. Valdés, G. Vargas, A. Sifeddine, L. Ortlieb and M. Guiñez, Distribution and enrichment evaluation of heavy metals in Mejillones Bay (23 S), Northern Chile: geochemical and statistical approach, *Marine Pollution Bulletin* **50** (2005), pp. 1558–1568.

Vargas et al., 2004 G. Vargas, L. Ortlieb, J.J. Pichon, J. Bertaux and M. Pujos, Sedimentary facies and high resolution primary production inferences from laminated diatomaceous sediments off northern Chile (23 S), *Marine Geology* **211** (2004), pp. 79–99

Vargas et al., 2007 G. Vargas, S. Pantoja, J.A. Rutllant, C.B. Lange and L. Ortlieb, Enhancement of coastal upwelling and interdecadal ENSO-like variability in the Peru–Chile current since late 19th century, *Geophysical Research Letters* **34** (2007), p. L13607

Zaragosi et al., 2006 S. Zaragosi, J.F. Bourillet, F. Eynaud, S. Toucanne, B. Denhard, A. Van Toer and V. Lanfumey, The impact of the last European deglaciation on the deep-sea turbidite systems of the Celtic-Armorican margin (Bay of Biscay), *Geo-Marine Letters* **26** (2006), pp. 317–329.

Zuta and Guillén, 1970 S. Zuta and O. Guillén, Oceanografía de las aguas costeras del Perú, Departamento de Oceanografía, *Boletín del Instituto del Mar del Perú* **2** (1970), pp. 193–196.

Zwolsman and Van Eck, 1999 J.J.G. Zwolsman and G.T.M. Van Eck, Geochemistry of major elements and trace metals in suspended matter of the Scheldt estuary, southwest Netherlands, *Marine Chemistry* **66** (1999), pp. 91–111.

Figures

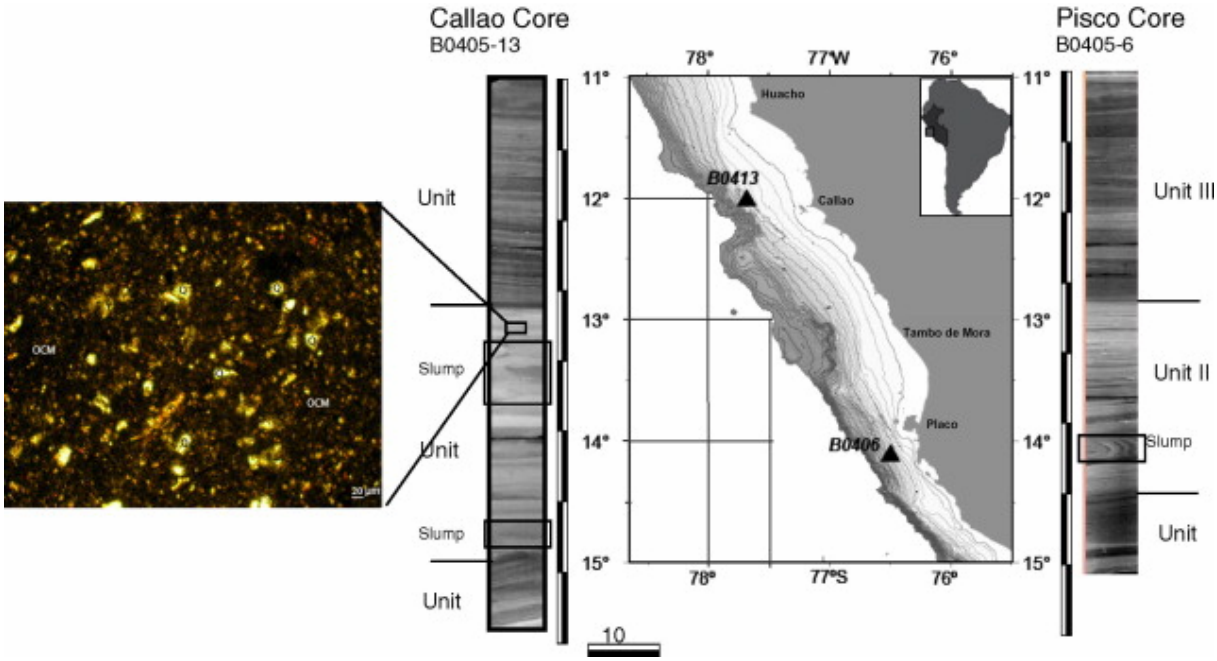

Fig. 1. Location and X-ray images of Pisco core (B0405-06, 14°07.90 S, 76°30.10W, 299 m depth) and Callao Core (B0405-13, 12°00′S, 72°42′S, 184 m depth) off the central-south Peruvian coast. Slumps are considered as instantaneous deposits, and are not considered in chronological development of downcore analyses. Light laminae are “dense”, dark laminae are “less dense”. The photograph shows the thin section of Callao core observed in polarized light. Q: quartz. F: feldspar, OCM: organic clay matrix.

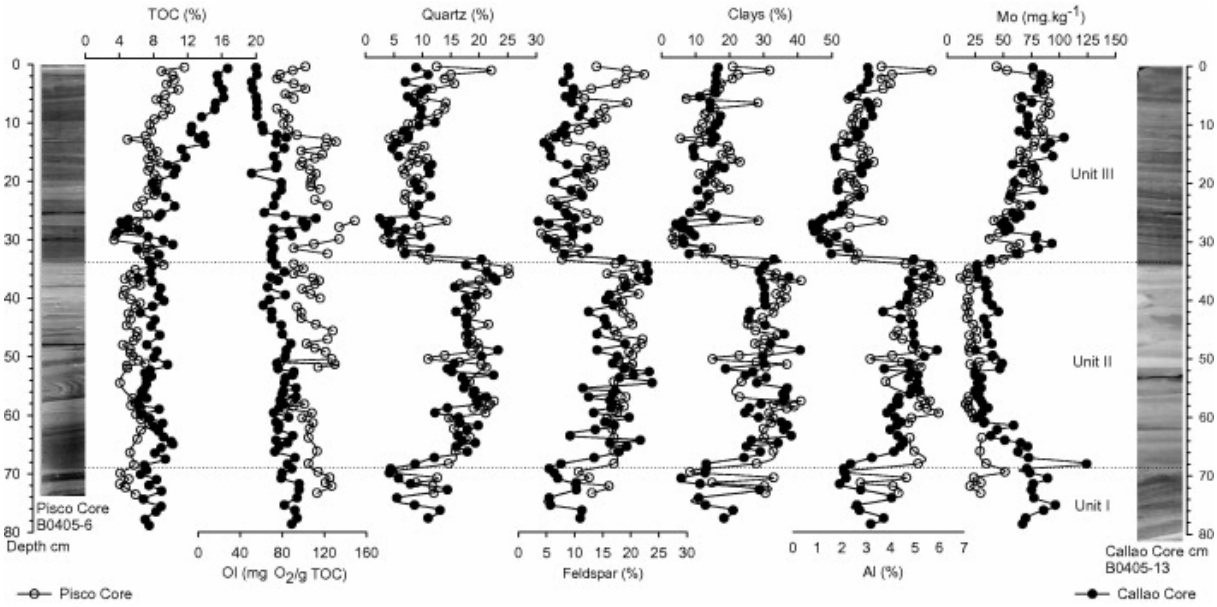

Fig. 2. Upcore variations of TOC content (%), IO (mg O_2/g TOC), mineral (quartz, feldspar) content, clays content, aluminium (%) and molybdenum content of Callao (black dots) and Pisco (open circles).

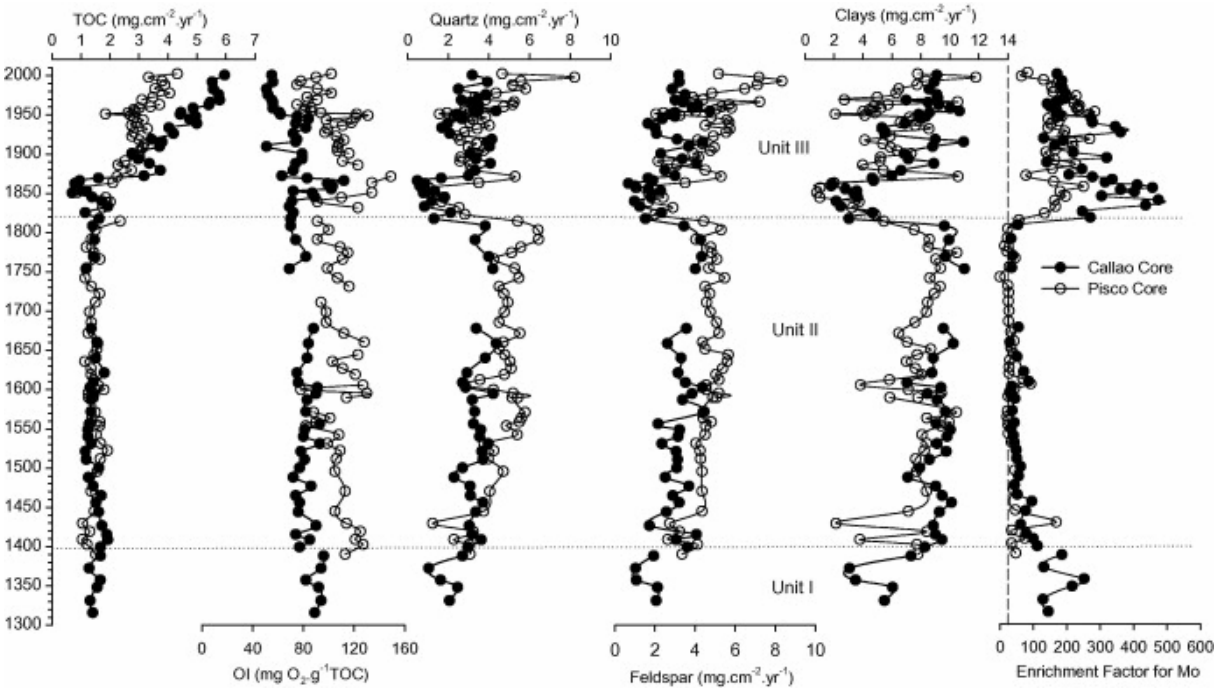

Fig. 3. Upcore variations of TOC fluxes, OI, mineral (quartz, feldspar, clays) fluxes, and EF for Mo of Callao (black dots) and Pisco (open circles).

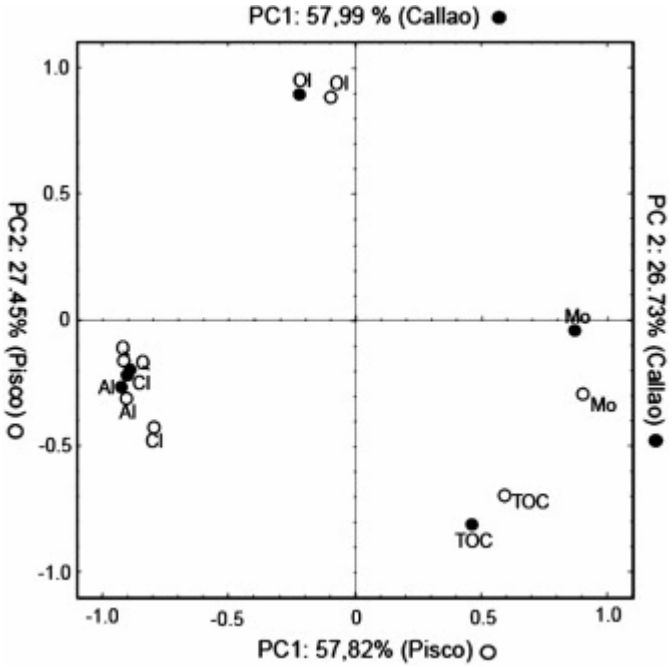

Fig. 4. Projection of the proxy variables on the factor-plane PC1 (quartz, feldspar and clays vs. TOC and Mo) in Callao (black dots) and Pisco (open circles) cores.

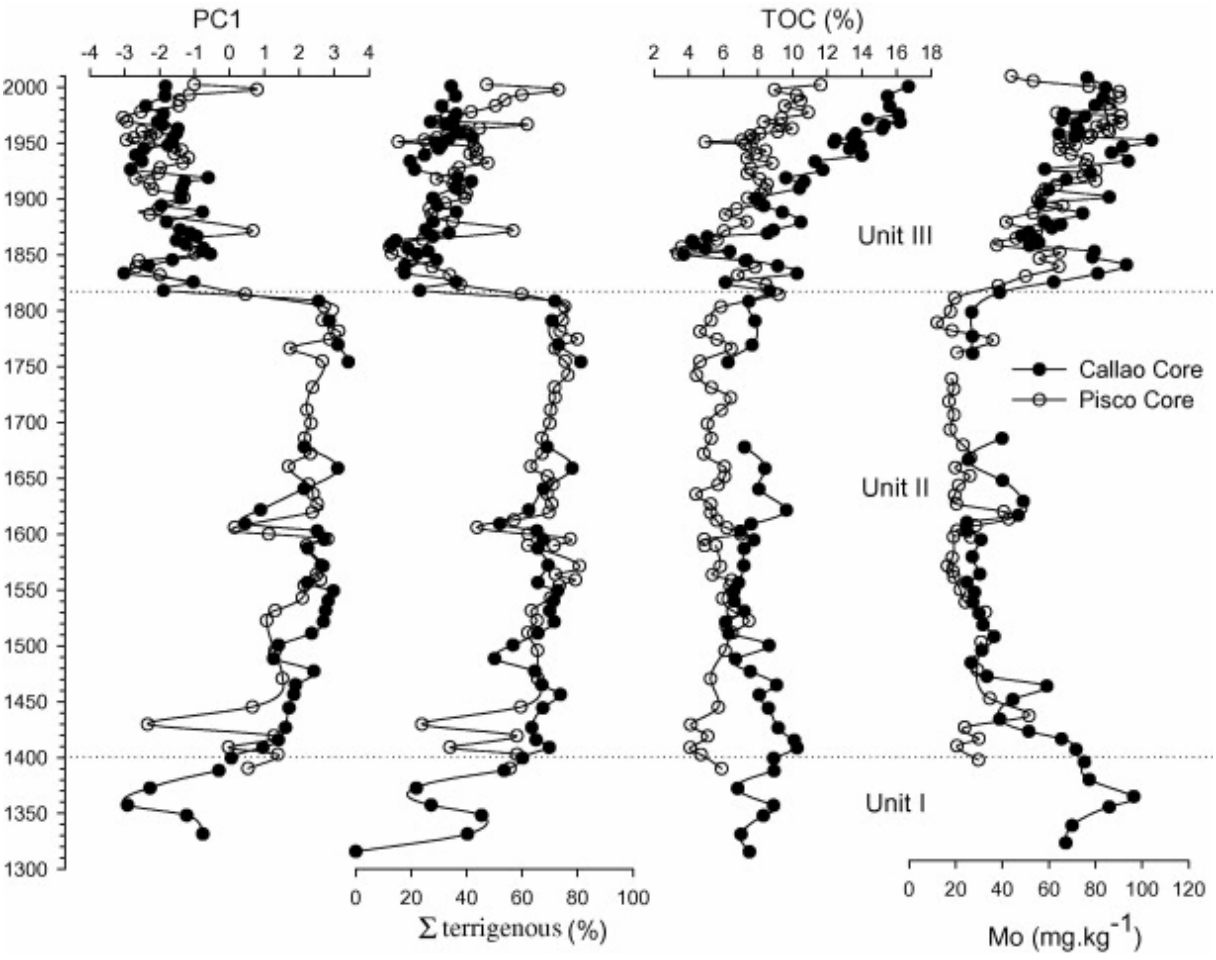

Fig. 5. Upcore variations of PC1, sum of the different terrigenous fractions, TOC and Mo content.

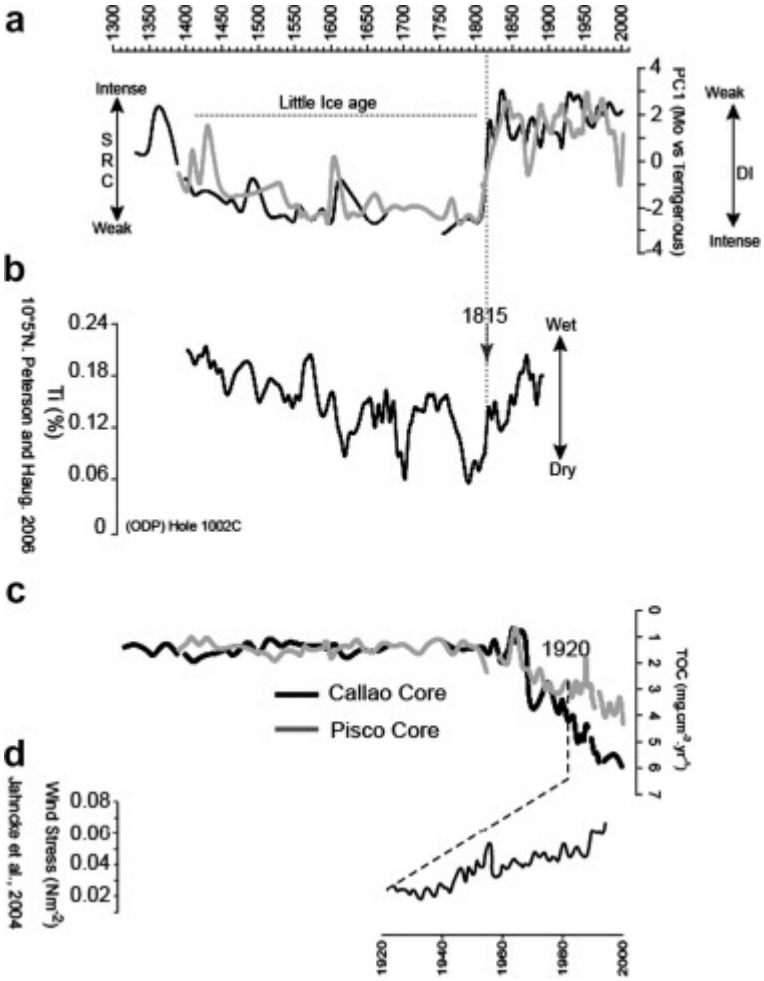

Fig. 6. Comparison between (a) PC1 upcore variation of Callao (black line) and Pisco (grey line), (SRC: sediment redox conditions; DI: detrital input. (b) Ti content of sediments from ODP Hole 1002C (record from Peterson and Haug, 2006), (c) TOC upcore variation of Callao (black line) and Pisco (grey line), (d) instrumental wind stress data from 1925 to 1995 (Jahncke et al., 2004).

Table

Table 1. : Geochemical and mineralogical measurements and their significance in paleoenvironmental reconstructions.

Proxies	**Environmental significance**
Mineral fraction (quartz, feldspar, clays)	Detrital input
Total organic carbon (TOC)	Productivity
Molybdenum (Mo)	Sediments redox conditions
Oxygen index (OI)	Degradation (aerobic oxidation)